

COMPARISON OF CYCLIC LOADING PROTOCOLS AND CYCLIC BENDING PERFORMANCES OF SELF-TAPPING SCREWS

Kenji Kobayashi¹, Keita Ogawa²

ABSTRACT: The load-displacement behavior of joints under cyclic loading is particularly important in seismic regions. There are several test standards for evaluating the shear performance of joints, as well as standards for bending tests of fasteners. However, the relationship between bending tests of fasteners and shear tests of joints is not clear. This study investigates the relationship between shear tests of joints and cyclic bending tests, focusing on the differences in loading histories in shear test methods. Cyclic shear tests of timber-to-timber joints using fully threaded screws and cyclic bending tests of fasteners under the same displacement history were conducted. Using low cycle bending fatigue parameters obtained from constant amplitude cyclic bending tests, the failure life of fasteners was estimated. The estimated failure life showed good agreement with the results of bending tests and shear tests of joints based on various test method standards.

KEYWORDS: screw, cyclic loading, low cycle fatigue, test method

1 – INTRODUCTION

The load-displacement behavior of joints under cyclic loading is particularly important in seismic regions. There are cyclic shear test standards such as ISO16670 [1], EN12512 [2], and ASTM E2126 [3] for evaluating the shear performance of joints. By conducting experiments according to these test standards, the shear performance of joints can be confirmed. On the other hand, there are cyclic bending test standards for fasteners themselves, such as JIS A1503 [4] and EN14592 [5], which allow for the evaluation of the low-cycle bending fatigue characteristics of fasteners. However, these test methods and requirements differ, and their relationship is not clear. Steilner [6] conducted shear tests of joints based on EN12512 using screws classified by performance through cyclic bending tests, and stated that using screws that showed high performance in cyclic bending tests improved the performance of joints. On the other hand, Schwendner [7] stated that cyclic bending tests could not predict the cyclic shear characteristics of hold-down joints. Nagase [8] demonstrated that the ultimate displacement of joints could be estimated from the low-cycle fatigue characteristics of fasteners by conducting cyclic bending tests at multiple amplitudes. However, since Nagase's study targeted loading histories with gradually increasing displacement, it is not clear whether it is effective for more

complex loading histories. Therefore, this study investigates the relationship between shear tests of joints and cyclic bending tests based on test method standards with different loading histories and attempts to estimate the failure life using the low-cycle fatigue characteristics of fasteners.

2 – CONSTANT AMPLITUDE CYCLIC BENDING TEST

2.1 – MATERIALS AND METHODS

To obtain the low cycle fatigue parameters of the fasteners, constant amplitude cyclic bending tests of the fasteners were conducted.

The fasteners used in the tests are shown in Fig. 1, and the testing machine in Fig. 2. The fastener used was a PX8-200 (manufactured by Synegic, nominal diameter 8 mm, length 200 mm). The testing machine used in the test was capable of cyclic bending tests as specified in JIS A1503.

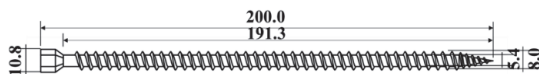
The fastener was fixed with the clamping jigs of the test machine, and cyclic bending tests under constant deformation angles were performed. The distance between the clamping jigs was set to 16 mm, which is twice the nominal diameter of the fastener. In this test, the load and deformation angle were measured. The load was measured

¹ Kenji Kobayashi, Graduate School of Agricultural and Life Sciences, The University of Tokyo, Tokyo, Japan, kobaken@g.ecc.u-tokyo.ac.jp

² Keita Ogawa, College of Agriculture, Academic Institute, Shizuoka University, Shizuoka, Japan, ogawa.keita@shizuoka.ac.jp

with a load cell (Shimadzu Corporation, TCLZ-500NA, 500N) attached to the end of the arm of the test machine, and the deformation angle was measured as a rotation angle of a rotating jig. The measured load was converted to moment by multiplying it by the distance from the load cell to the failure position of the fastener. In this research, cyclic bending tests were performed with three target angles of $\pm 13^\circ$, $\pm 22.5^\circ$, and $\pm 30^\circ$. The number of test specimens was 16 for the 13° test, 12 each for the 22.5° and 30° tests. The test was terminated after the cycle in which the measured load became nearly zero. A definition of the plastic deformation angle $\Delta\gamma_p$ is shown in Fig. 3. In this research, $\Delta\gamma_p$ was determined as the x-coordinate of the intersection point of the moment-deformation angle curve and the x-axis, at the unloading phase of first positive and negative cycles.

A half cycle ($2N_f$) is defined by counting the number of the movement between positive and negative peaks until a peak moment decreases less than 80% of maximum moment. It is not counted when moving from point “a” from “o” in Fig. 3 but becomes 1 when reaching point “b” from “a”. Thereafter, 1 is added for each positive and negative peak experienced. The number of cycles N_f is defined as the half cycle divided by 2. According to JIS A1503, the number of cycles (N_{f_JIS}) is counted as 1 at the initial positive peak (point “a”), and 1 is added when reaching the positive peak again after passing the negative peak (point “b”). Therefore, it is equivalent to adding 1 to N_f in this study.



Unit: mm

Figure 1. Definition of plastic deformation angle

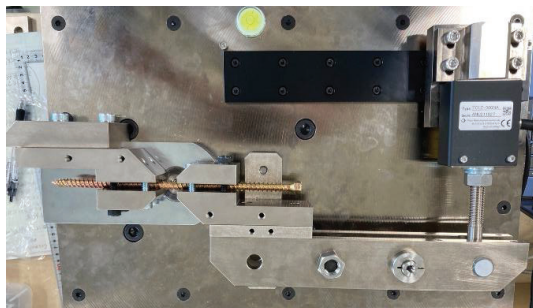


Figure 2. Definition of plastic deformation angle

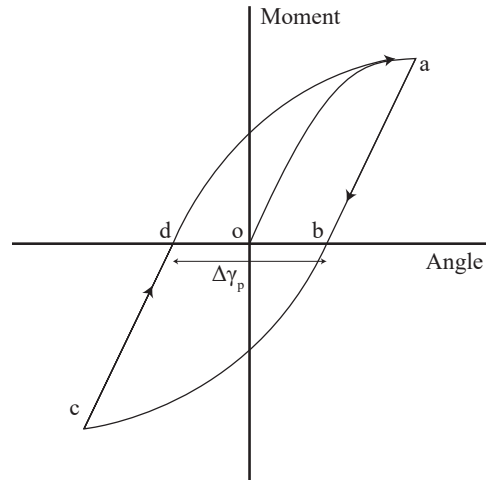


Figure 3. Definition of plastic deformation angle

2.2 – RESULTS AND DISCUSSION

Representative moment-deformation angle relationships obtained in the test are shown in Figs. 4-6. Many repetitions were required to reach failure at small deformation amplitudes. In this test method, no backlash behavior (slip behavior when the moment becomes zero) was observed. The characteristic values obtained from the test are shown in Table. 1. $\Delta\gamma_p$ increased as the deformation angle increased, while N_f tended to decrease.

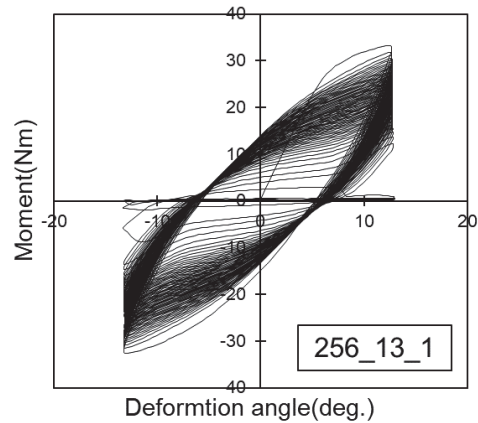


Figure 4. Example of Moment deformation angle relationship (13 deg.)

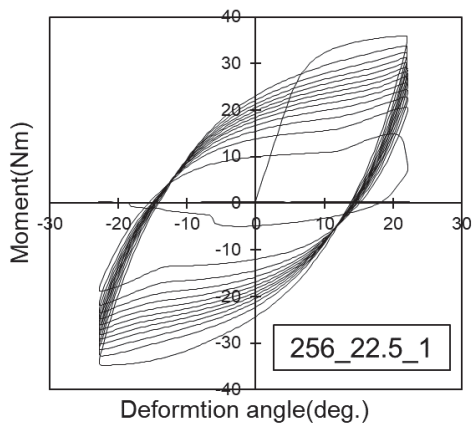


Figure 5. Example of Moment deformation angle relationship (22.5 deg.)

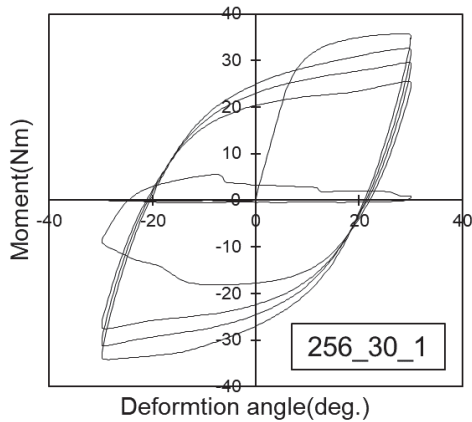


Figure 6. Example of Moment deformation angle relationship (30 deg.)

Table 1. Characteristic values of cyclic bending test

Deformation angle deg.	M_{max} Nm	γ_p deg.	N_f
13	33.34 (0.56)	5.20 (0.26)	19.50 (1.85)
22.5	35.24 (0.51)	13.78 (0.32)	5.21 (1.03)
30	35.70 (0.53)	21.32 (0.41)	2.13 (0.30)

The relationship between plastic deformation angle and the number of bending cycles until failure is shown in Fig. 7. The results show linear relationships on a logarithmic graph. These regression equations will be used at the next chapter.

JIS A5559(2023) requires that screws should withstand 7 or more cycles at a plastic deformation angle of 7° (not less

than $0.8M_{max}$), which means $2N_f \geq 12$ and $\Delta\gamma_p/2 = 7$ deg. EN14592(2022) has two criteria during 3 cyclic loading at an angle α_c and monotonic loading. We assumed that $N_f \geq 6$ and $\Delta\gamma_p/2 = \alpha_c - \gamma_{el}$ (γ_{el} : elastic deformation angle) as an alternative criterion for comparison. Fig. 4 shows relationship between $\Delta\gamma_p/2$ and $2N_f$ of the screw used for the test and two standards. Criteria of these standards can be plotted on the figure.

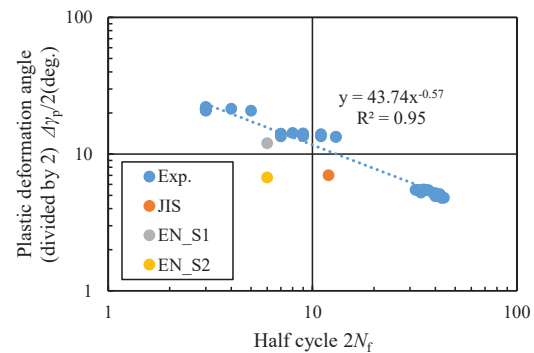
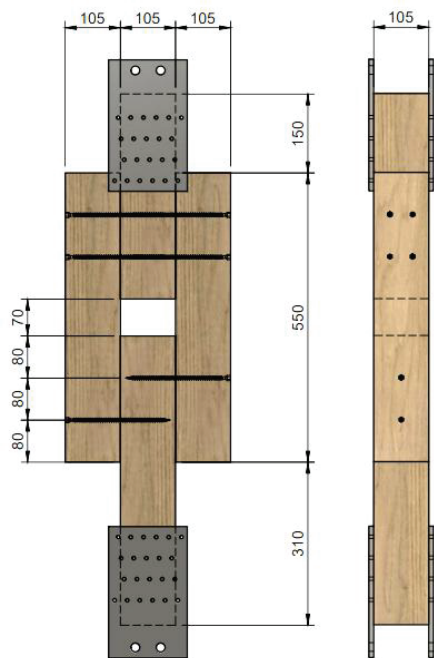


Figure 7. Relationship between half cycle and plastic deformation angle

3 – JOINT SHEAR TEST AND FASTENER BENDING TEST ACCORDING TO SEVERAL LOADING PROTOCOLS

3.1 – MATERIALS AND METHODS

Homogeneous grade glulam (Japanese Cedar, E65-F255) was used for main and side member. Screws used for the test were the same (PX8-200) as in Chapter 2. The test specimen is shown in Fig. 8. The dimensions of the timber were 105 x 105 x 550 mm for side members and main member of the lower part of the test specimen, and 105 x 105 x 390 mm for the main member of the upper part of the test specimen. A pilot hole with a diameter of about 4 mm and a depth of about 40 mm was drilled in the side wood to allow the screws to drive straight through.



Unit: mm

Figure 8. Joint test setup

A monotonic loading test was conducted to determine the yield displacement and ultimate displacement which is used to determine the loading history. A single test specimen was used, and the test was terminated when the load decreased to 80% of the maximum load after the maximum load was reached.

Each characteristic value was calculated by applying an energy equivalent elastic-plastic (EEEP) model to the load-displacement relationship obtained from the joint test. The evaluation method using the EEEP model is shown in Fig. 9. A line connecting the loads corresponding to 10% and 40% of the maximum load P_{max} was drawn (line 1). Next, the points corresponding to $0.4P_{max}$ and $0.9P_{max}$ were connected (line 2). A line parallel to line 2 was drawn so that it becomes tangent to the load-displacement curve (line 3). The yield load P_y is defined as the load at the intersection of line 1 and line 3, and the displacement on the load-displacement curve at load P_y is defined as the yield displacement D_y . A line connecting the origin and the point (D_y, P_y) is defined as line 4, and its slope is defined as the initial stiffness K . The ultimate displacement D_u is defined as the displacement when the load decreases to 80% of the maximum load after reaching the maximum load. Additionally, a line parallel to the Y-axis passing through D_u is defined as line 5. The area enclosed by the X-axis, the load-displacement curve, and line 5 is defined

as S . Line 6 is determined so that the area enclosed by the X-axis, line 4, line 5, and line 6 parallel to the X-axis is equal to S . Here, the load value of line 6 is defined as the ultimate strength P_u , and the displacement at the intersection of line 4 and line 6 is defined as the yield point displacement D_v . Furthermore, the plasticity ratio μ is calculated as D_u / D_v .

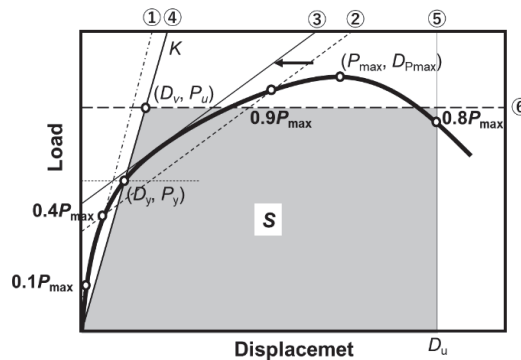


Figure 9. Energy equivalent elastic-plastic model

Loading histories used for the tests are shown in Fig. 10. Three types of loading histories were used: the loading history based on ISO16670 (hereinafter referred to as ISO), the CUREE loading protocol (ASTM E-212610) Method C) (hereinafter referred to as CUREE), and the Sequential-Phased Displacement loading protocol (ASTM E-2126 Method A) (hereinafter referred to as SPD). The ISO loading history is based on the ultimate displacement D_u of the monotonic loading test (25mm). It repeats cycles of 1.25%, 2.5%, 5%, 7.5%, and 10% of D_u one each, and then repeats three cycles of gradually increasing the displacement by 20%, such as 20%, 40%, 60%, 80%, 100%, 120%, etc. CUREE is also based on the ultimate displacement D_u of the monotonic loading test. Six cycles of 5% of D_u are repeated, one cycle of 7.5% ($0.075D_u$), six cycles of 75% of $0.075D_u$, one cycle of 10% of D_u ($0.1D_u$), and six cycles of 75% of $0.1D_u$. After that, one cycle of $0.2D_u$, three cycles of 75% of $0.2D_u$, one cycle of $0.3D_u$, three cycles of 75% of $0.3D_u$, one cycle of $0.4D_u$, two cycles of 75% of $0.4D_u$, one cycle of $0.7D_u$, two cycles of 75% of $0.7D_u$, one cycle of $1.0D_u$, two cycles of 75% of $1.0D_u$, one cycle of 20% increase, and two cycles of 75% of each are repeated. SPD is a loading history based on the yield displacement D_v of a monotonic loading test (9.8mm). Cycles of 25%, 50%, and 75% of D_v are repeated three times each. After that, a cycle of 100% of D_v is repeated once, and cycles of 75%, 50%, and 25% of 100% are repeated once each, and finally a cycle of 100% of D_v is repeated three times (hereinafter, this group of cycles is called a phase). This phase is repeated at $100+5\mu\%$ of D_v .

(μ : plasticity ratio of unidirectional loading test), 100+10 μ %, 100+20 μ %, 100+40 μ %, and thereafter at values that increase by 20 μ %.

The deformation angle history of the bending test for the fastener was obtained using the displacement history from the joint test and the following equation.

$$\theta = \tan^{-1} \left(\frac{\delta}{L} \right) \quad (1)$$

where θ : deformation angle of the fastener, δ : displacement of the joint test, L : distance between rotation centers.

The distance between rotation centers L in (1) was calculated based on the failure mode theory. The failure mode theory includes six failure modes, and for each failure mode, the yield load P_y is calculated, adopting the failure mode with the smallest P_y . As a result of the joint test, all specimens in this study were in mode IV, so the formula for mode IV was used to calculate the distance between rotation centers L . The formula used is shown in (2).

$$L = \frac{1}{\beta} \sqrt{\frac{4\beta M_p(\beta+1)}{F_c d}} \quad (2)$$

where M_p : a full plastic moment of the fastener (N·mm), F_c : a bearing strength of the main member (N/mm²), β : a ratio of bearing strength of the side member to the main member.

M_p and F_c were obtained from material test. Since the main member and the side member are made of the same material, β is 1.

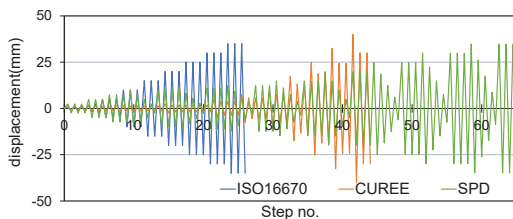


Figure 10. Loading protocols

3.2 – RESULTS AND DISCUSSION

Examples of moment deformation angle curves in fastener bending tests with different loading histories are shown in Figs. 11-13, and examples of load-displacement curves in joint tests are shown in Figs. 14-16. In both tests, differences in loading histories resulted in varying strength

and deformation performance. In the bending tests, high moment and deformation performance were observed under ISO conditions. When the history at small deformation angles increased, failure occurred at smaller deformation angles. In the joint tests, the ultimate displacement D_u value was higher under CUREE conditions.

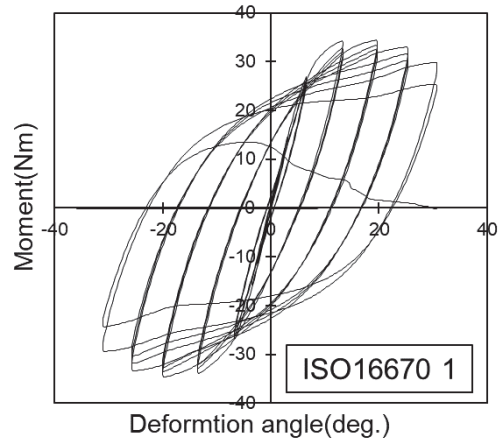


Figure 11. Example of moment deformation angle relationship (bending, ISO)

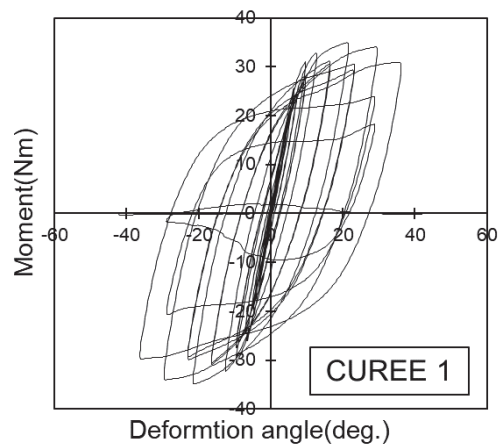


Figure 12. Example of moment deformation angle relationship (bending, CUREE)

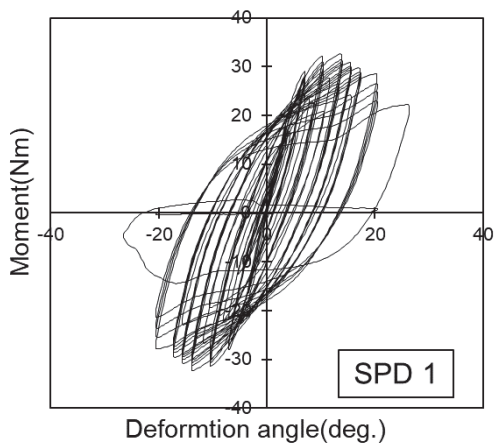


Figure 13. Example of moment deformation angle relationship (bending, SPD)

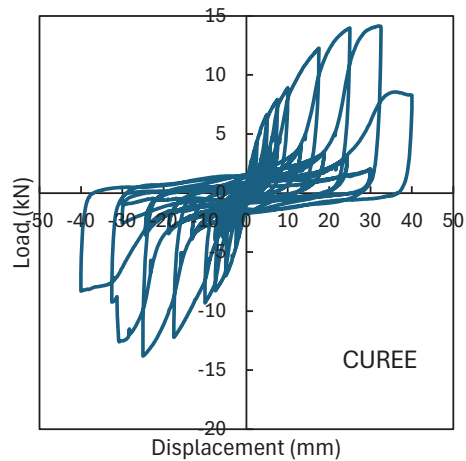


Figure 15. Example of load displacement relationship (joint, CUREE)

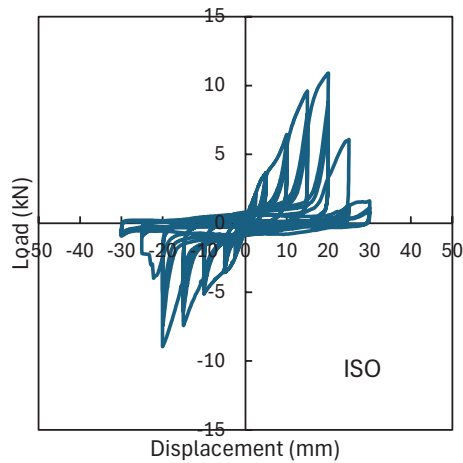


Figure 14. Example of load displacement relationship (joint, ISO)

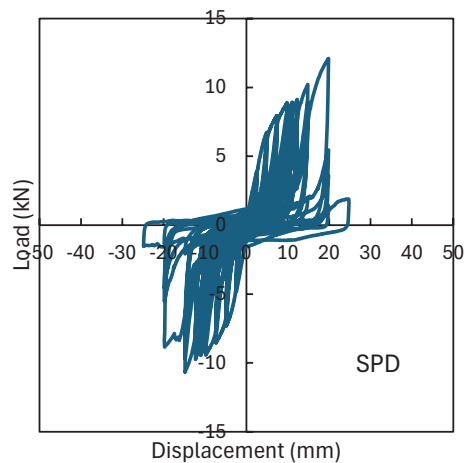


Figure 16. Example of load displacement relationship (joint, SPD)

3.3 – ESTIMATIO OF FAILURE LIFETIME

Failure lifetime was estimated based on Nagase [8]. Low cycle fatigue parameters of the screw were determined according to constant amplitude cyclic bending tests. Definition of plastic deformation angle $\gamma_p/2$ and number of cycles to failure $2N_f$ are shown in Figure 3. A test method according to JIS A1503 provide results without any slip at zero moment. A half cycle N_f is counted at point “a” and “c”. Relationship between $\gamma_p/2$ and $2N_f$ is expressed as:

$$\frac{\Delta\gamma_p}{2} = \gamma_f \cdot (2N_f)^C \quad (3)$$

where: γ_f , C : regression coefficients. These values were determined by Fig. 7.

Miner's rule is shown in equation (4). The number of cyclic bending repetitions until fatigue failure at a specific deformation angle is denoted as N_i , and it is obtained by substituting the plastic deformation angle into equation (3). If the history at that deformation angle is repeated n_i times, the damage degree can be expressed as n_i / N_i . The sum of the damage degrees at each deformation angle is denoted as D , and fatigue failure is considered to occur when this value reaches or exceeds 1.

$$D = \frac{n_1}{N_1} + \frac{n_2}{N_2} + \dots + \frac{n_i}{N_i} = \sum \frac{n_i}{N_i} \quad (4)$$

3 – RESULT AND DISCUSSION

Estimated and experimental step number at failure are shown in Figure 17. The numbers at failure were similar between joint test and fastener bending test. In ISO protocol, the numbers were smaller than other protocols because ISO protocols reach to large displacement in small step number (Figure 10). The results of the fastener bending tests and the joint shear tests are generally consistent, although there are some differences caused by a variance of timber members. Estimated failure life showed good agreement with the fastener bending test and joint test results.

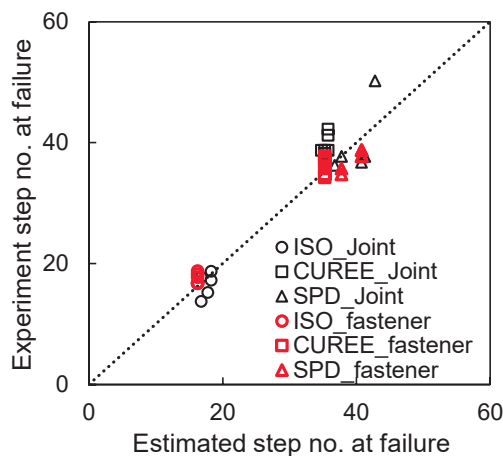


Figure 17. Estimated and experimental step number at failure

4 – CONCLUSION

This study investigates the relationship between shear tests of joints and cyclic bending tests, focusing on the differences in loading histories in shear test methods. Cyclic shear tests of timber-to-timber joints using fully threaded screws and cyclic bending tests of fasteners under the same displacement history were conducted. Using low cycle bending fatigue parameters obtained from constant amplitude cyclic bending tests, the failure life of fasteners was estimated. The estimated failure life showed good agreement with the results of bending tests and shear tests of joints based on various test method standards.

5 – REFERENCES

- [1] ISO 16670: Timber structures – Joints made with mechanical fasteners – Quasi-static reversed-cyclic test method, 2003.
- [2] EN 12512 + A1: Timber structures – Test methods – Cyclic testing of joints made with fasteners. CEN, 2005.
- [3] ASTM E2126: Standard Test Methods for Cyclic (Reversed) Loading Test for Shear Resistance of Walls for Buildings, American Society for Testing and Materials, 2005.
- [4] JIS A1503: Test methods for screw for timber structure, Japanese Standards Association, 2022.
- [5] EN 14592: Timber structures – Dowel-type fasteners – Requirements, CEN, 2022.
- [6] Steilner M. et al.: Low cycle ductility of self-tapping screws. INTER 55-7-5, Bad Aibling, Germany, 2022.
- [7] Schwendner S. et al. : Low cycle fatigue of self-tapping screws. INTER 56-7-2, Biel/Bienne, Switzerland, 2023.
- [8] Nagase, K., et al. : Estimation of failure lifetime in plywood-to-timber joints with nails and screws under cyclic loading. Journal of wood science, DOI 10.1007/s10086-018-1742-8, 2018.
- [9] JIS A5559: Screws for timber structure, Japanese Standards Association, 2023.